

Morphological, Mechanical and Thermal Characteristics of PLA /*Cocos nucifera L* Husk and PLA/*Zea mays* Chaff Lignin Fibre Mats Composites

O. P. Gbenebor^{1*}, C.C. Odili², V.D. Obasa³, E.F. Ochulor¹, S.O. Kusoro¹, O.C. Udogu-Obia¹,
S.O. Adeosun^{1,4}



¹Department of Metallurgical and Materials Engineering, University of Lagos, Nigeria.

²Department of Biomedical Engineering, Bells University of Technology, Ota, Nigeria

²Department of Mechanical Engineering, Edo State University Uzairue, Iyamho, Nigeria.

³Department of Industrial Engineering, Durban University of Technology, Durban, South Africa.



ABSTRACT: Polylactide (PLA) is a biodegradable polymer with low elongation which limits its use in some applications. The incorporation of biowaste particles has been employed to improve its properties. This work thus examines the impact of lignin particles reinforced on electrospun PLA fibre mats. Acid hydrolysis (1M of HCl at 60 and 100 °C for 2 and 4 h) was used to extract lignin from *Cocos nucifera L* (CNHL) and *Zea Mays* Chaff (CCL). Lignin particles were added to molten PLA, stirred, and electrospun at 26 kV, using a static aluminum collector plate placed at 121mm from the spinneret tip. Morphological examination reveals that fibre diameter of neat PLA (9.7 µm) increased from 107 – 285 % with the additions of reinforcements. Maximum tensile strength of 1.03 MPa is recorded for PLA/CNHL 60 °C/ 2 h. This composite maintains the highest elongation of 0.069 % compared to neat PLA (0.046 %). X-Ray diffractometer (XRD) result informs that the crystallinity of neat PLA (67.6 %) improves by 3%, with the use of CNHL 60 °C/ 2 h. Thermo gravimetric analysis (TGA) result shows that both fibre composites possess better thermal stability (380 °C) compared to reinforcing PLA fibre (319 °C).

KEYWORDS: Biomass, electrospinning, fibre, lignin, polylactide

[Received Jan. 14, 2023; Revised June 19, 2023; Accepted Oct. 21, 2023]

Print ISSN: 0189-9546 | Online ISSN: 2437-2110

I. INTRODUCTION

The global mass from agricultural waste is approximately over 150 billion/years, with about 10% used for energy production (Morganti, 2015). Lignocellulose is the major structural component of woody and non-woody plants. A huge amount of these wastes is generated through forestry, agricultural practices, timber industries, bioethanol fuel production, pulp and paper industry (Obielodan *et al.*, 2019; Wang *et al.*, 2019). As a global practice, majority of them are disposed via burning and this causes environmental pollution. These wastes, however, can be converted into value-added products such as biofuel, energy source for fermentation, and precursors for carbon fibre (Howard, *et al.*, 2003). Lignin makes up to 10-25 % of lignocellulosic biomass. It is the second most abundant natural polymer after cellulose (Hu, *et al.*, 2011; Min *et al.*, 2013). Lignin is made up of three dimensional highly cross-linked macromolecules consisting of *p*Coumaryl, *cn*iferyl and *sn*apyl alcohols (Morganti and Stroller, 2017).

The structure possessed by lignin has facilitated its use as reinforcements in composite materials; when in particle form, it can improve mechanical and thermal stabilities of polymers (Hilburg *et al.*, 2014). One of such polymers is PLA – a hydrophobic biodegradable biopolymer that can be obtained from sugarcane and corn starch (Vink *et al.*, 2004). This

polymer can be used as an implant (Adeosun *et al.*, 2014) and wound dressers (Akpan *et al.*, 2019). Hydrophobicity of PLA has been reduced with the use of palm kernel shell (Gbenebor *et al.*, 2018) and bagasse particles (Akpan *et al.*, 2019). Polylactide is highly brittle (elongation is less than 10 %) with very low toughness (Auras *et al.*, 2004); therefore, there is a need to improve on its tensile properties through the use of plant-based reinforcement like coconut husk (CNHL) and corn chaff lignin (CCL). Spiridon and Tanase (2018) blended PLA pellets with soft wood lignin at 175 °C to form bio-composites of desired shapes via compression molding. It was observed that beyond 7 wt. % lignin reinforcement, the tensile strength of PLA was significantly improved owing to plasticizing effect of lignin. Pirani *et al.* (2013) electrospun PLA/Nanocrystalline cellulose (NCC) based composites and showed that at 1% NCC, the percentage elongation at fracture of the composite slightly improved to 4.23% relative to unreinforced PLA (4.19%). Obielodan *et al.* (2019) characterized PLA/Lignin for 3D printing and the results revealed that the initial percentage elongation of PLA (4.24 %) was increased to 6.85 % with the addition of 15wt. % lignin to PLA matrix. One of the techniques used in producing Polymer-lignin composite is electrospinning, which offers a quick and fast way of producing fibrous scaffold. It is also known as systematic method of fabricating fibres into nano and micro scale (Ruiz-Rosas *et al.*, 2010). Investigations have reported the influence of lignin (from various sources) on the

*Corresponding author: ogbenebor@unilag.edu.ng.

mechanical properties of PLA via different production routes. To the best of our knowledge, there is little or no work on the use of CNHL and CCL to improve the tensile properties of electrospun PLA. Therefore, this work examines the morphology, crystallinity, thermal and tensile characteristics of the PLA/Lignin spun fibre mats.

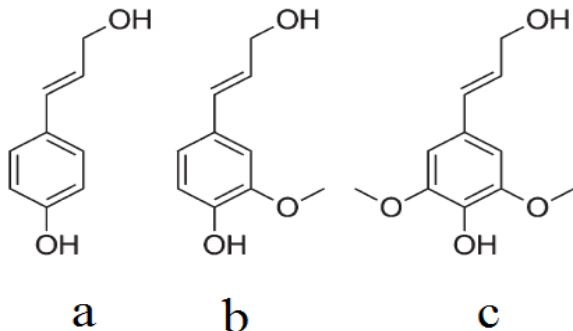


Figure 1 : (a) *p*Coumaryl (b) Cniferyl and (c) sinapyl alcohols (Stanley *et al.*, 2013)

II. MATERIALS AND METHODS

A. Materials

Poly lactide of 250,000 g/mol average molecular weight was purchased from Nature Works, China. Dichloromethane (DCM) 95% purity and HCl 37% purity with a specific gravity of 1.18 were obtained from Sigma-Aldrich, USA. Distilled water was obtained from the distiller in Metallurgical and Materials Engineering, Laboratory, University of Lagos, Lagos, Nigeria.

B. Lignin extraction

The corn chaff used for this study was the waste obtained from the sieving of soaked and ground corn seeds. The corn seeds were softened by soaking for 5 days at room temperature, washed, and blended to fine particles with the use of an electric blending machine. The blended corn was sieved to separate the chaff from the starch. The coconut husk (*Cocos nucifera L*) used was obtained from coconut fruit. The corn chaff and coconut husk were washed with distilled water to eliminate impurities; they were sun-dried for 2 days at ambient temperature. Fibres from the coconut husk were removed, ball milled, and sieved to 150 μ m particle size. Forty grams of corn chaff and coconut husk were weighed and soaked in 1M HCl solution. The delignification process was carried out in a water bath at 60 and 100^o C for 2 and 4 h at each extraction temperature. The solution was filtered to neutrality and the residue (lignin) was oven dried at 80 ^oC for 5 h. Lignin sourced from coconut husk and corn chaff are designated CNHL and CCL respectively in this study.

C. PLA dissolution and Electrospinning Process

Poly lactide pellets (6.5 g) was dissolved in 0.5 ml DCM at room temperature. After complete dissolution, 0.5 g each of CNHL and CCL particles were separately added to the PLA solution and continuously stirred to achieve a uniform

distribution of particles in the PLA matrix. The solution was withdrawn into a 20 mL syringe (used as a spinneret in this study) which was connected to a 26 kV voltage source. The spinneret was positioned upright at 90^o to a stationary aluminum collector plate placed at 121mm from its (spinneret) tip.

D. Tensile test

Tensile strength characteristics of the neat PLA and the composites mats (30mm x 50mm) were determined using Instron model 313 Tensometer, bluehillTM version 1.00 software located at Centre for Energy Research and Development, Obafemi Awolowo University, Ile-Ife, Nigeria. Each of the samples was fixed and held firmly at both ends by the gauge as the load was applied until the sample finally fractured. Generally, PLA reinforced with CNHL and CCL extracted at 60 and 100 ^oC for 2 h displayed good response under tensile loading than those obtained at 4 h. Fibre mat of PLA/CCL and PLA/CNHL extracted at 60 and 100 ^oC for 2 h was thus selected for further characterizations due to enhanced mechanical performance.

E. Scanning Electron Microscopy (SEM) analysis

The samples' micrographs were produced via a scanning electron microscopy model Phenom Eindhoven, Netherlands situated at Ahmadu Bello University, Zaria, Nigeria. It operated with an electron intensity beam of 15 kV while the samples were mounted on a conductive carbon imprint left by the adhesive. Samples were placed on a circular holder and coated for 5 min to enable it to conduct electricity. Free online software, Image J was used to determine the pore size and fibre diameter of electrospun mats.

F. X-Ray Diffraction (XRD) analysis

The X-ray diffractometry measurements were performed using an EMPYERN diffractometer model XRD-600, at the National Geosciences Research Laboratory, Kaduna. The facility used CuK α radiation ($\lambda=1.540598$ nm, Ni-filter) at 40kv, 30mA. Without any preferred orientation, the samples were scanned in steps of 0.026261 in the 2θ in the range of 4.99 - 75 using a count time of 29.7s per step. The crystallinity index (Crl) for the neat PLA and the composites mats were calculated using Segal method (Tian *et al.*, 2014).

$$\text{Crl}(\%) = \left[\frac{I_{002} - I_{am}}{I_{002}} \right] \times 100 \quad (1)$$

Where I_{002} and I_{am} represent the maximum intensities of approximately 16.7^o and the minimum intensity respectively.

G. Thermogravimetric Analysis (TGA)

Analysis of samples was carried out on TGA Q500 instrument, where 2 mg of samples were heated to 750 ^oC at 10 ^oC/ minute. The temperature for the onset of thermal decomposition (T_{onset}), temperature at the end of decomposition (T_{finish}) and the temperature at which

decomposition was maximum (T_{max}) were deduced from the thermograms.

III. RESULTS AND DISCUSSION

A. Tensile test result

The tensile performance of the electrospun PLA/lignin fibre mat is shown in Figure 2. The tensile strength of PLA is enhanced by the addition of lignin to the polymer mix. The tensile strength of neat PLA (0.19 MPa) improves to 0.3 and 1.03 MPa on reinforcement with CCL/60 °C/ 2 h and CNHL/60 °C/ 2 h respectively. The findings in this work is in agreement with Spiridon and Tanase, (2018) and Wang *et al.*, (2012) where an increase in the tensile properties of PLA reinforced with lignin was reported; the improvement was attributed to the plasticizing effect of lignin. Polylactide reinforced with CNHL/60 °C/ 4 h and CCL/60 °C/ 4 h show poor tensile performance with a tensile strength of 0.12 MPa for CCL and 0.025 MPa for CNHL recorded. Singla *et al.*, (2016) observed the tensile strength of PLA-reinforced lignin to decrease with an increase in lignin content. The decrease was attributed to the formation of hydrogen bonding between the hydroxyl group of lignin and the carboxyl group of the PLA matrix, which could contribute to matrix immobilization in the interlayer. The tensile strength reported in this work is within the range (0.99 - 1.35 MPa) reported by Salami *et al.*, (2017) for randomised polycaprolactone (PCL) and lignin composite fibre mat. They also reported that the tensile strength of PCL reduced with an increase in the weight fraction of lignin. In this present study, it is observed that the tensile strength of PLA is enhanced on reinforcing with CNHL and CCL, which may be ascribed to better interfacial interaction between the lignin and PLA matrix. Similarly, Kai *et al.* (2015) reported an increase in the tensile strength of electrospun PCL/Lignin-PMMA (polymethyl methacrylate). It was reported that the improvement in the grafted PMMA chains on the lignin surface, which facilitated better interfacial bonding between lignin particles and the PCL matrix, was responsible for the tensile strength improvement.

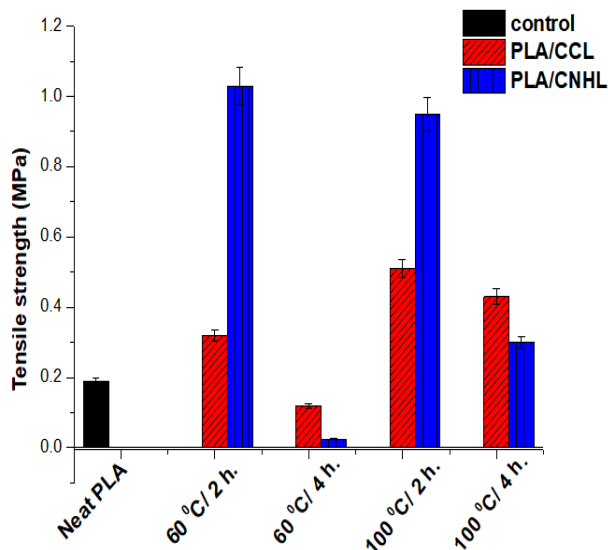


Figure 2: Tensile strength of electrospun PLA/lignin fibre mats

The fracture stress of PLA and its composites is shown in Figure 3, where the fracture stress of PLA is 0.018 MPa. Maximum fracture stress of 0.51 MPa was attained with PLA/CNHL/60 °C/2 h. There is a 44-344 % improvement in fracture stress of neat PLA (0.018 MPa) when reinforced with lignin. The enhanced fracture stress could be attributed to the control interfacial bond between lignin reinforcement and PLA matrix as stated in Ogunbiyi *et al.*, (2022).

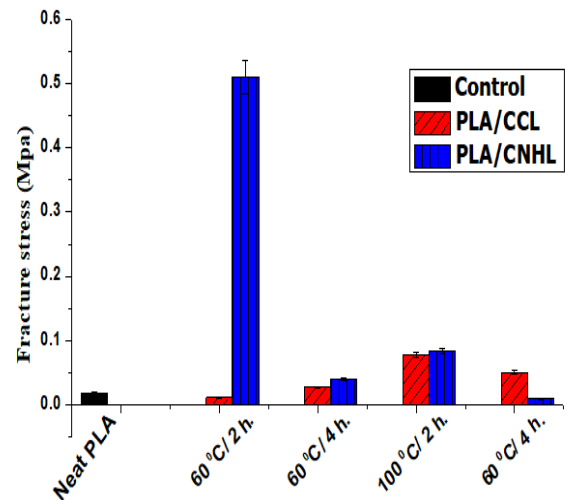


Figure 3: Fracture stress of electrospun PLA and PLA/lignin fibre mats

Elongation at the break for the composites in comparison with the unreinforced PLA (0.046 %) prior to fracture is shown in Figure 4. The composite shows 0.043, 0.069, 0.030, 0.028, 0.018, 0.029, 0.018 and 0.028 % for PLA/CCL 60 °C/2 h, PLA/CNHL60 °C/2 h, PLA/CCL60 °C/4 h, PLA/CNHL60 °C/4 h, PLA/CCL100 °C/2 h, PLA/CNHL100 °C/2 h, PLA/CCL100 °C/4 h) and PLA/CNHL100 °C/4 h respectively. The highest elongation (0.069 %) is attained with PLA/CNHL/60 °C/2 h. Gordobil *et al.*, (2015) reported improvement in PLA/lignin composite elongation after extrusion as the unreinforced PLA (2.2%) improved to about 3.2 and 4 % when reinforced with 0.5 and 5wt. % of acetylated kraft lignin (AKL).

However, at a higher percentage of AKL, the ductility decreased. The improvement was attributed to the esterification of esters which acted as a plasticizer. The reduced elongation at the break of composites compared to unreinforced PLA in this study may be due to the inhomogeneous distribution of lignin within which will restrict the movement of the PLA chain the PLA matrix, which will restrict the movement of the PLA chain. The mobility of the polymer's molecular chain was restricted and this made the material stiff.

The elastic modulus of PLA, PLA/CCL60 °C/2 h, PLA/CNHL60 °C/2 h, PLA/CCL (60 °C/ 4 h, PLA/CNHL60 °C/4 h, PLA/CCL100 °C/2 h, PLA/CNHL100 °C/2 h, PLA/CCL100 °C/4 h and PLA/CNHL100 °C/4 h are 5.7, 9.5, 49, 3.7, 5.2, 27.2, 36.9, 23.1 and 2.9 MPa respectively (Figure

5). Composites PLA/CCL60 °C/4 h (3.7 MPa), PLA/CNHL60 °C/4 h (5.2 MPa), and PLA/CNHL100 °C/4 h (2.9 MPa) show low modulus of elasticity compared to unreinforced PLA (5.7 MPa).

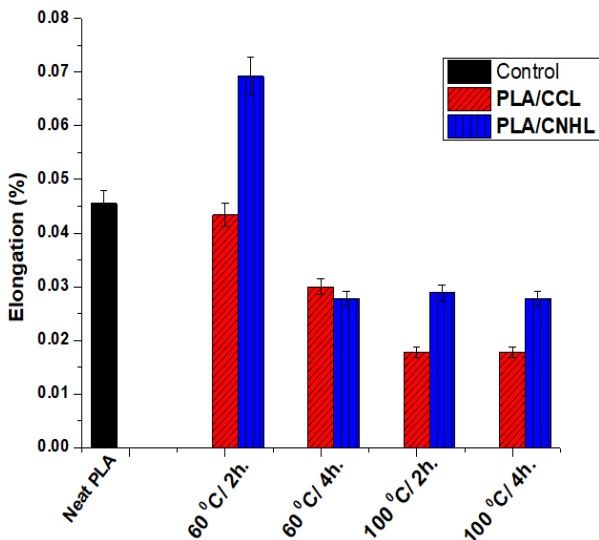


Figure 4: Elongation of PLA/Lignin electrospun fibre mats

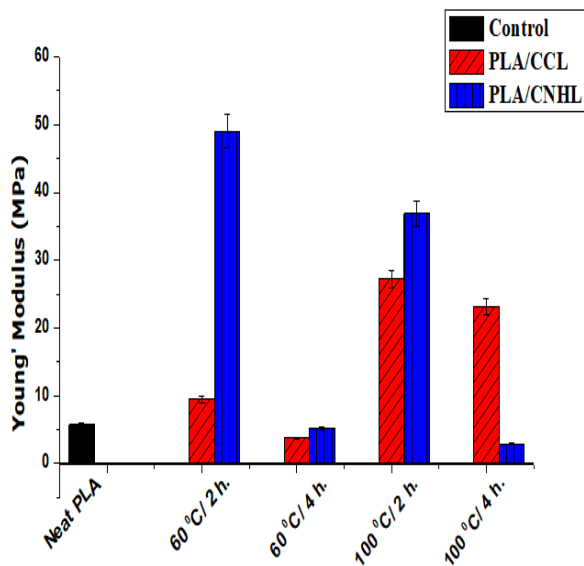
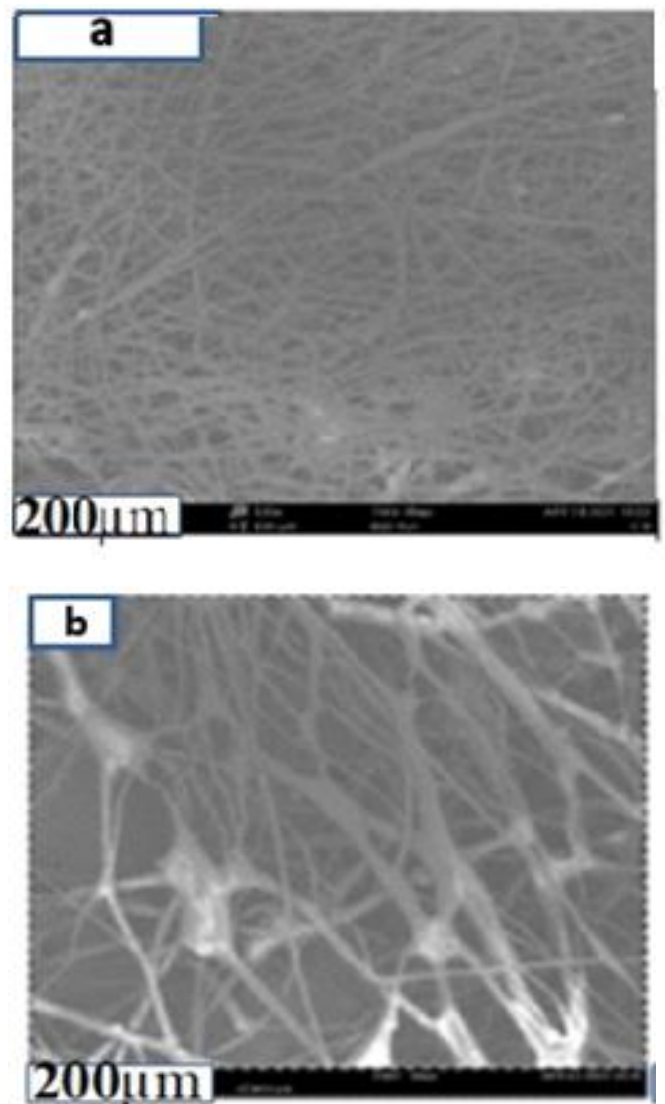


Figure 5: Young's Modulus of PLA/Lignin electrospun fibre mats

B. Scanning Electron Microscopy result

The morphology of the neat PLA electrospun fibre mat (Figure. 6a) shows a randomly oriented fibre without a bead. Composite PLA/CCL60 °C/ 2 h. (Figure 6b) shows a good fibrous network, resembling that of an extracellular cell matrix (ECM) with pores that can facilitate tissue ingrowth. Figure 6c reveals encapsulated lignin fibre while Figure 6d shows a poor fibre formation. The average fibre diameter (Figure 7) of a neat PLA mat is 9.7 µm. On reinforcement with CCL and CNHL, the fibre diameter increases to 20.1 and 23 µm respectively for 60 °C/2 h, while at 100 °C/2 h, it increases to

37 and 34 µm respectively. The fibre diameter of the mat increases with an increase in the processing temperature of lignin used in reinforcing PLA. In general, PLA/CCL60 °C/2 h has the smallest diameter. The average pore size (Figure 8) of neat PLA measures 43 µm upon the addition of lignin treated at 60 °C/2 h; the average pore sizes of 69 and 22 µm are measured for PLA/CCL and PLA/CNHL respectively at 100 °C/2 h. Composites PLA/CCL and PLA/CNHL have average pore sizes of 23 and 25 µm, respectively. It is important to note that pore size requirements for scaffolds vary according to tissues and transplanted cells. Composites PLA/CNHL 60 °C/2 h, PLA/CCL, and PLA/CNHL both at 100 °C/2 h are suitable for endothelial cells, whose pore size ranges between 10-25 µm (Wang *et al.*, 2016); cells less than 38 µm are affirmed to be the best for microvascular epithelial cells. In addition, neat PLA and PLA/CCL 60 °C/2 h with 20-100 µm pore size, could also serve as a scaffold for nerve cells (Wang *et al.*, 2016). It can thus be deduced that CCL-reinforced PLA has a better average than PLA/CNHL variant. It can be suggested that PLA/CCL would make a better scaffold than PLA/CNHL. Furthermore, CCL and CNHL extracted at 60 °C/2hr are good reinforcements for PLA/lignin fibre.



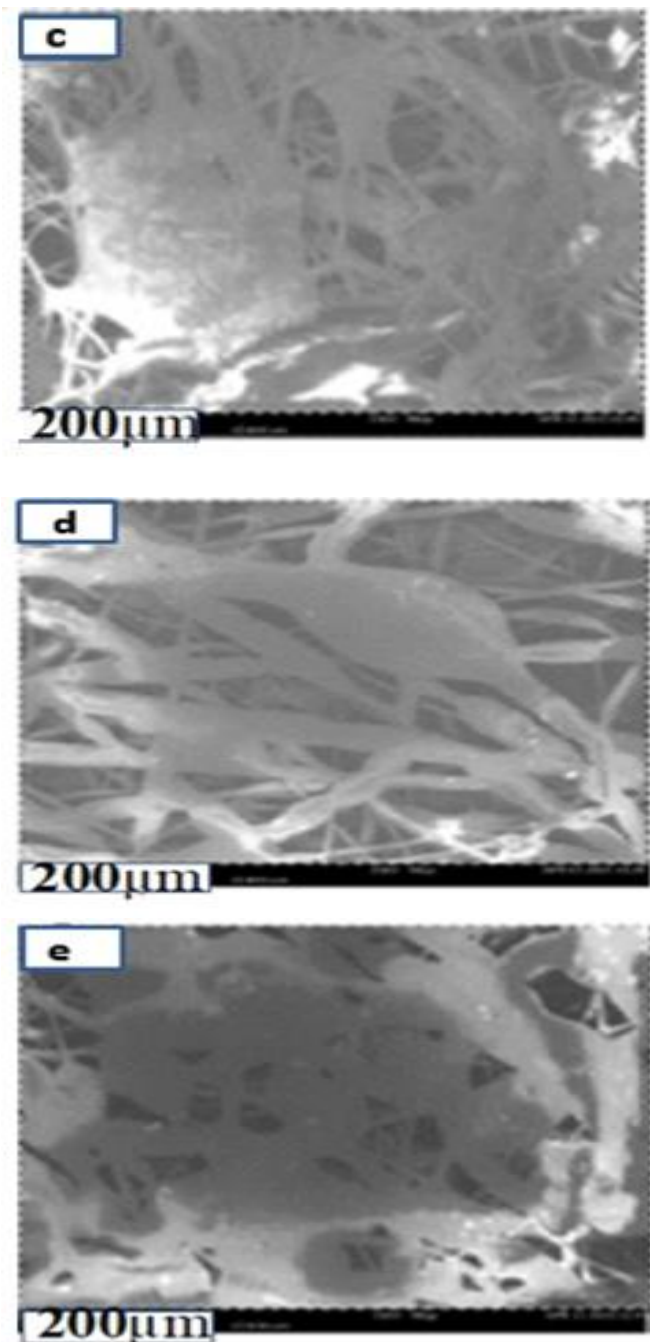


Figure 6: Morphology of electrospun fibre mats (a) neat PLA (b) PLA/CCL60 °C/ 2 h (c) PLA/CCL100 °C/ 2 h (d) PLA/CNHL both at 60 °C/2 h (e) PLA/CNHL both at 100 °C/2 h

C. X-Ray Diffraction

The XRD patterns of neat PLA, and PLA/lignin fibre mats (PLA reinforced with CCL and CNHL at 60°C/ 2 h and 100 °C/ 2 h) are shown in Figures 9 and 10 respectively. Two strong peaks are observed at $2\theta = 16.2$ and 20.1° , which represent the crystalline peaks of PLA and lignin respectively. Fibre mat of PLA /CCL shows higher intensity compared to PLA /CNHL fibre mat extracted at 60 °C/ 2 h. A similar diffractogram (Figure 10) is also observed for the lignin extracted at 100 °C/ 2 h. A broader peak at the same 2θ position (16.2 and 20.1°) is, however, observed. Comparing

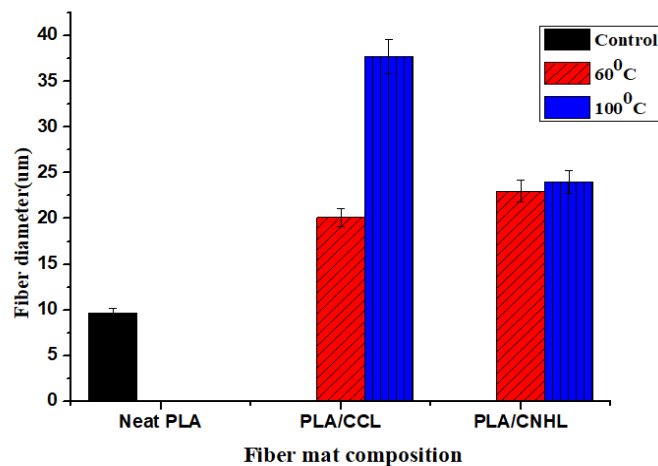


Figure 7: Fibre diameter of electrospun fibre mats

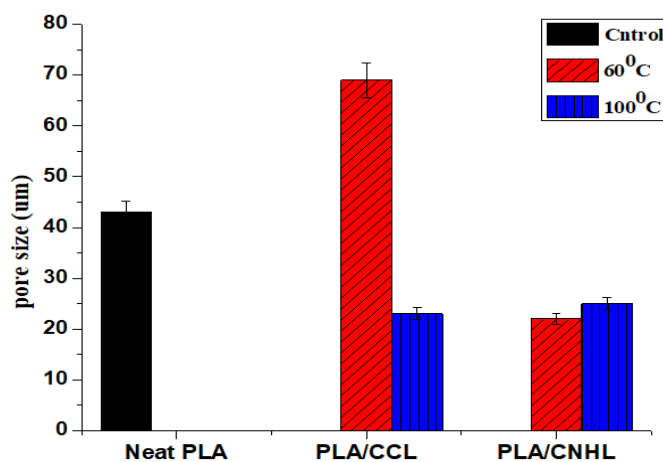


Figure 8: Pore sizes of electrospun fibre mats.

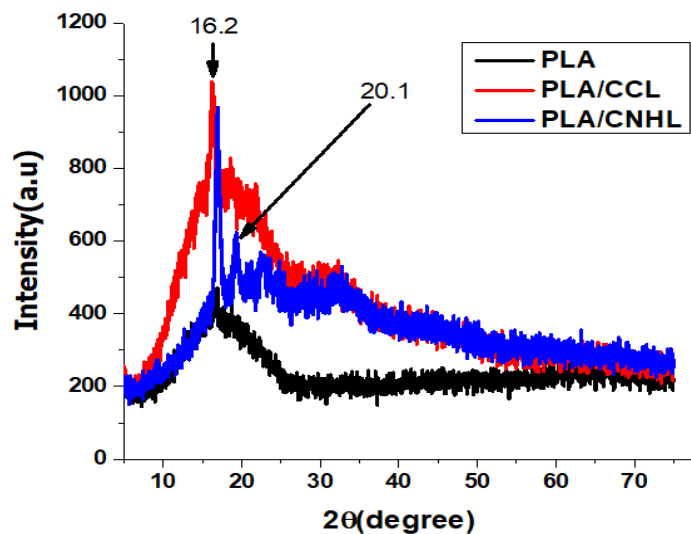


Figure 9: XRD of electrospun PLA/Lignin fibre mat at 60 °C/ 2 h

the crystallinity of PLA/lignin fibre mat extracted at 60 and 100 °C/ 2 h (Table 1), the crystallinity of PLA /CCL/60 °C/ 2 h and PLA /CNHL/60 °C/ 2 h are 69.8 and 70 %, respectively. Similarly, the fibre mat of lignin extracted at 100 °C/ 2 h

exhibits crystallinity of 66 and 65 % for PLA /CCL/100 °C/ 2 h and PLA /CNHL100 °C/ 2 h respectively.

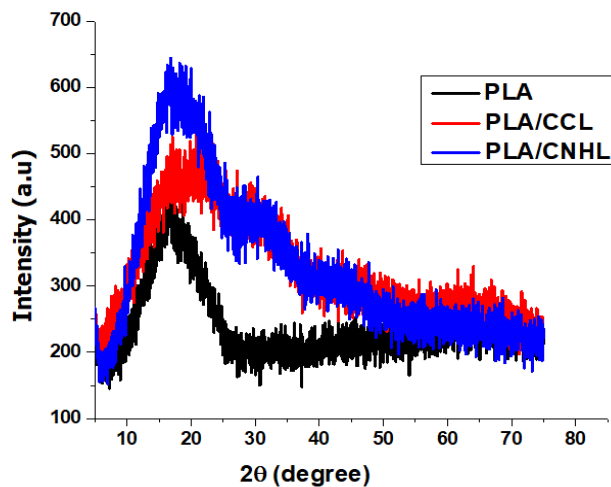


Figure 10: XRD of electrospun PLA/lignin fibre mat at 100 °C/ 2 h

Table 1: Crystallinity of the electrospun PLA/lignin fibre

	Crystallinity (%)	
Fibre mat	60°C/ 2 hr	100°C/ 2 hr.
Neat PLA	67.6	67.6
PLA/CCL	69.8	66.0
PLA/CNHL	70.0	65.0

D. Thermogravimetric Analysis

The thermograms of electrospun PLA /CCL and PLA /CNHL fibre mats at 60 °C/ 2 h and 100 °C/ 2 h are shown in Figures 11 and 12, respectively. The thermogram of electrospun PLA/lignin fibre mat at 60 °C/ 2 h, shows three stages of decomposition. The first weight loss occurred around 140 °C, which is attributed to the loss of volatile materials such as moisture (Bernabe *et al.*, 2013). The second degradation that occurred between 210 and 380 °C is the degradation of lignin. The weight loss at this stage is due to the thermal degradation of carbohydrate and aliphatic groups present in the lignin, which leads to the formation of CO, CO₂ and CH₄.

At this point, there is degradation of lignin complex structure such as fragmentation of inter unit linkage between phenolic hydroxyl (OH), carbonyl (C=O) and phenolic groups (C₆H₆O), releasing monomeric phenols into the vapour phase (Sun *et al.*, 2001). The final stage is between 380 and 460 °C, which represents the temperatures of commencement and end of PLA decomposition. Beyond this temperature, there exists disintegration of volatile products from lignin such as aldehydes, alcohols and acids degrade and are separated (Attia *et al.*, 2021). The degradation temperature of PLA is noted to be within 320- 331 °C as reported by Ainali *et al.*, (2021) and Nur *et al.*, (2019). Information from the thermogram also reveals that the thermal stability of PLA is improved by reinforcing it with lignin (336 °C).

This result was also ratified by Khoo *et al.*, (2015), where they used nanocellulose to improve the thermal stability of PLA. The improvement on thermal property of PLA/lignin composite can be attributed to the presence of OH and aromatic phenyl group (Spiridon *et al.*, 2015). The DTG of

PLA/CCL and PLA/CNHL show a maximum decomposition temperature of 416 and 369 °C, respectively for lignin extracted at 60 °C for 2 h. Similarly, electrospun fibre mat extracted at 100 °C for 2 h show 398 and 446 °C for PLA/CCL and PLA/CNHL, respectively. Comparing electrospun fibres mats with neat PLA (Figure 13), a single stage PLA decomposition with no lignin evidence was observed to commence from 319 °C. The reduced temperature of onset of decomposition implies that the thermal stability of neat electrospun PLA fibre is lower than the lignin-reinforced fibres.

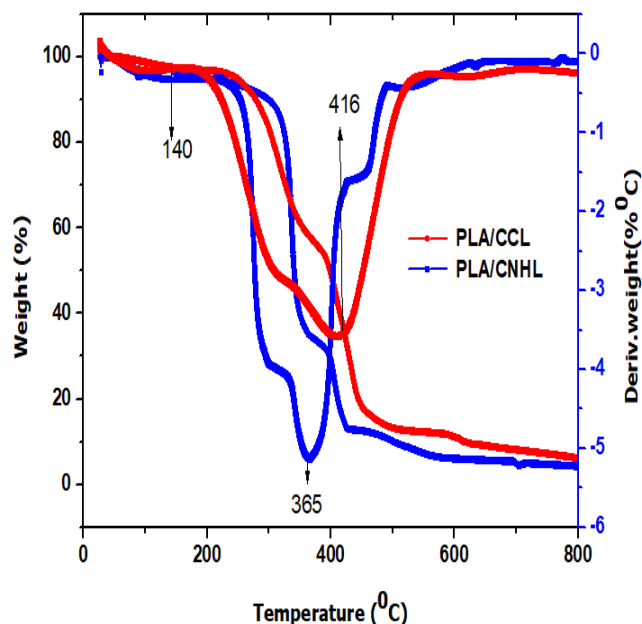


Figure 11: TGA/DTG of electrospun PLA/Lignin fibre mat 60°C/ 2 h

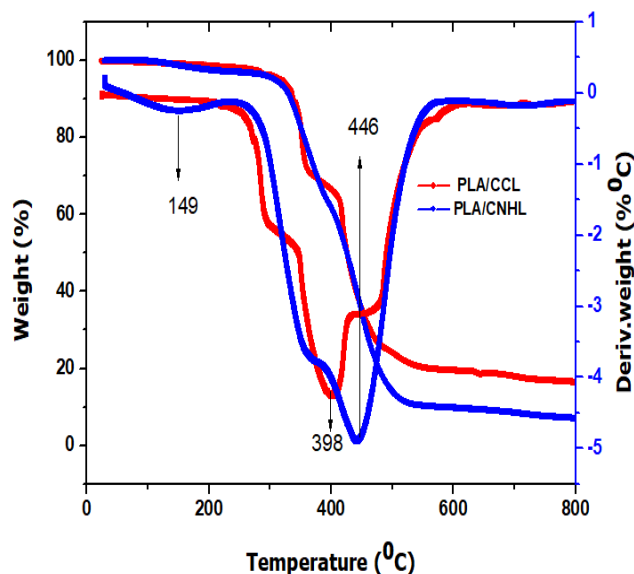


Figure 12: TGA/DTG of electrospun PLA/Lignin fibre mat 100 °C/2h

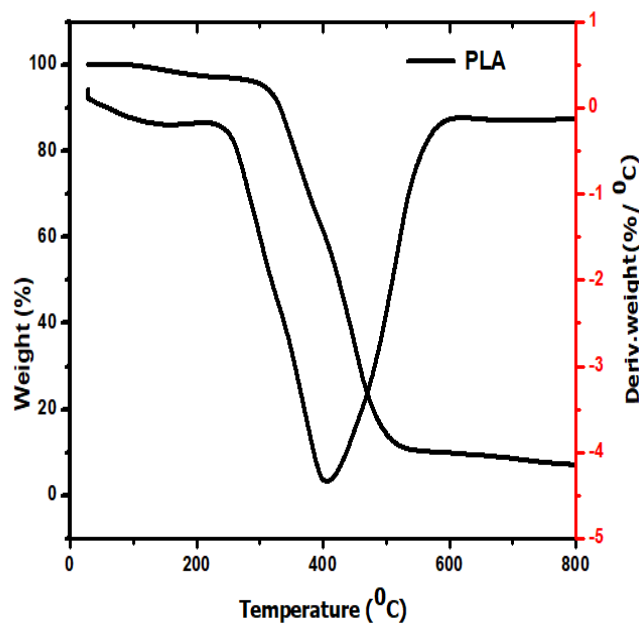


Figure 13: TGA/DTG of electrospun PLA fibre mat

IV. CONCLUSION

Electrospun PLA/lignin fibre mats have been produced and characterised in this study. Morphological examination of PLA/CCL60 °C/ 2 h spun fibre mat shows superior fibre network and pore space resembling that of extracellular matrix (ECM). This makes it potentially useful for tissue engineering applications. The pore space of PLA (43µm) is improved by 60 %, when reinforced with CCL processed at 60 °C for 2 h (PLA/CCL60 °C/2 h). The pore spaces will allow tissue ingrowth and cell proliferation. The pore space reported here is within the range of scaffold for nerve cells (20-100 µm). Furthermore, the crystallinity of PLA/CCL and PLA/CNHL fibre mat is approximately the same (70 %). Both reinforcements have played a major role in improving the tensile properties of the electrospun PLA fibre mats. Reinforcing PLA with CNHL and CCL can thus be considered as bio-composites for tissue engineering due to the enhanced pore space with improved ductility they have displayed.

AUTHOR CONTRIBUTIONS

Gbenebor O.P. - Conceptualization; Data curation; Formal analysis; Investigation; Methodology; Project administration; Resources; Writing - review & editing; **Odili, C.C.** - Methodology, Writing - original draft; **Obasa, V.D.** - Methodology; **Ochulor, E.F.** - Methodology, Investigation; **Kusoro, S.O.** - Methodology; **Udogu-Obia, O.C.** - Methodology; **Adeosun, S.O.** - Conceptualization; Investigation; Methodology; Project administration; Supervision, review & editing.

REFERENCES

Adeosun, S.O.; G.I. Lawal and O.P. Gbenebor. (2014). Characteristics of Biodegradable Implants. *Journal of*

Minerals and Materials Characterization and Engineering, 2: 88-106.

Ago, M.; K. Okaima; J.E. Jakes; S. Park and O.J. Rojas. (2012). Lignin Base Electrospun Nano Fibres Reinforced with Cellulose Nanocrystals. *Biomacromolecules*, 13:918-926.

Ainali, N.M.; E. Tarani; A. Zamboulis; K.P. Crsnar; L.F. Zemljic; K. Chrissafis; D.A. Lambropoulou and D.N. Bikiaris. (2021). Thermal Stability and Decomposition Mechanism of PLA Nanocomposites with Kragt Lignin and Tannin. *Polymers*, 13(16): 1-16.

Akpan, E.I.; O.P. Gbenebor; E.A. Igogori; A.K. Aworinde; S.O. Adeosun and S.A. Olaleye (2019).. Electrospun Bio-Fibre Mat Based on Polylactide / Natural Fibre Particles. *Arab Journal of Basic and Applied Sciences*, 26(1):225-235.

Attia, A.A.M.; K.M. Abas; A.A.A. Nada; M.A.H.Shouman; A.O. Siskova and J. Mosnacek. (2021). Fabrication, Modification and Characterization of Lignin-Based Electrospun Fibers Derived from Distinctive Biomass Sources. *Polymers*, 13 (2277): 1-28.

Auras, R.; B. Harte. and S. Seke. (2004). An Overview of Polylactide as Packaging Materials. *Molecular Bioscience*, 4: 835-864.

Bernabe, G.A.; M. Kobelnik; S. Almeida; C.A. Ribeiro and M.S. Crespi. (2013). Thermal behaviour of lignin and cellulose from waste composting process, *Journal of Thermal Analysis and Calorimetry*, 111 (1):589-595.

Borrego, M.; J.E. Martin-Alfonso; M.C. Sanchez; C. Valencia and J.M. Franco. (2021). Electrospun Lignin-PVP Nanofibers and their Ability for Structuring Oil. *International Journal of Biological Macromolecules*. 180:212-221.

Cui, M.; N.A. Nguyen; P.V. Bonnesen; D. Urig; J.K. Keum and A.K. Naskar. (2018). Rigid Oligomer from Lignin in Designing of Tough Self-Healing Elastomers. *ACS, Macro letter*, 7: 1328-1332.

Gbenebor, O.P.; E.I. Akpan; R.A. Atoba; S.O. Adeosun; S.A. Olaleye; O.O. Taiwo; E.A. Igogori; O.B. Alam and A.K. Aworinde. (2018). Development and Performance Analysis of High Voltage Generator for Electrospinning of Nanofibres. *Unilag, Science Journal Medicine and Technology*, 6(2): 45-58.

Gordobil, O.; R. Delucis; L. Egues and J. Labidi. (2015). Kraft Lignin as a Filler in PLA to Improve Ductility and Thermal Properties. *Industrial crops and products*, 72: 46-53.

Honarbaksh, S. and Pourdeyhimi. B. (2011). Scaffold for Drug Delivery. Part1: Electrospun Porous Poly (lactic acid) and Poly (Lactic Acid)/Poly (Ethylene Oxide) Hybrid Scaffolds. *Journal of materials science*, 46(9): 2874-2881.

Howard, R.L.; E. Abotsi; E.L.J. Rensburg and S. Howard. (2003). Lignocellulose Biotechnology: Issues of Bioconversion and Enzyme Production. *African Journal of Biotechnology*, 2(12):602-619.

Hu, L.; H. Pan; Y. Zhou and M. Zhang. (2011). Methods to Improve Lignin Reactivity as a Phenol Substitute and Replacement for other Phenolic Compounds: A Brief Review. *Bioresources*, 6(3):3515-3525.

- Hilburg, S.L.; A.N. Elder; H. Chung; R.L. Ferebee; M.R. Bockstaller and N.R. Washburn. (2014).** A Universal route Towards Thermoplastic Lignin Composites with Improved Mechanical Properties. *Polymer*, 55(4): 995-1003.
- Kai, D.; J. Shan; Z.W. Low and X.J. Loh. (2015)..** Engineering Highly Stretchable Lignin-Based Electrospun Nanofiber for Potential Biomedical Application. *Journal of Material B*, 3(30): 6194-6204.
- Khoo, R.Z.; H. Ismail and W.S. Chow. (2015).** Thermal and Morphological Properties of Poly (Lactic Acid)/Nanocellulose Nanocomposites. 5th International conference on Recent Advances in Materials, Minerals and Environment (RAMM) and 2nd International Postgraduate Conference on Materials, Minerals and Polymer (MAMIP), 4-6 August. Nibong tebal, Malaysia.
- Kumar, M.; M. Hietala and K. Oksman. (2019).** Lignin-based Electrospun Carbon Nanofibers. *Frontiers in Materials*. 6(62):1-6.
- Min, D.; S.W. Smith; H. Chang, and H. Jameel.(2013).** Influence of Isolation Condition on Structure of Milled Wood Lignin Characterized by Quantitative ¹³C Nuclear Magnetic Resonance Spectroscopy. *Bioresources*, 8(2): 1790-1800.
- Morganti, P. (2015).** Biotechnology and Bioeconomy for a Greener Development, *Journal of Applied Cosmeotology*, 33:51-3365.
- Morganti, P. and Stroller, M. (2017).** Chitin and Lignin: Natural Ingredients from Waste Materials to Make Innovative and Healthy Products for Human and Plant. *Chemical Engineering Transactions*, 60: 319-324.
- Narayan, D. and Venkatraman, S.S. (2008).** Effect of Pore Size and Interpore Distance on Endothelial Cell Growth on Polymers. *Journal of Biomedical Materials Research Part A*, 87A(3):710-718.
- Nur, A.S.; Z.M. Abdullah; H.C.M. Siti; B. Northarina; A.M. Rohah; J. Mazura and N. Norzita. (2019).** Thermal and toughness Enhancement of Poly (Lactic Acid) Bionanocomposites. *Chemical Engineering Transactions*, 72: 427-432.
- Obielodan, J.; K. Vergenz; D. Aqil; J. Wu and L. McElistrem.(2019).** Characterization of PLA/Lignin Biocomposites for 3D Printing. *Proceedings of the 30th Annual International Solid Freeform Fabrication Symposium- An Additive Manufacturing Conference*, 998-1007.
- Ogunbiyi, O.; O.P. Gbenebor; S.Saliu; S. Olaleye; T. Jamiru; R. Sadiku and S. Adeosun, (2022).** Strength characteristics of electrospun coconut Fibre Reinforced Poly(lactic Acid): Experimental and Representative Volume Element (RVE) Prediction. *Materials*, 15(19):1-15.
- Pirani, S.; H.M.N. Abushammala and R. Hashaikeh. (2013).** Preparation and Characterization of Electrospun PLA/Nanocrystalline Cellulosa Based Composites. *Journal of Applied Polymer Science*, 130:3345-3354.
- Ruiz-Rosas, R.; Bedia, J.; M. Lallave; L.G. Liscwerales; A. Barrero; J. Rodriguez-Miraso and T. Coredo. (2010).** The Production of Submicron Diameter Carbon Fibers by Electrospinning of Lignin Carbon, 48: 696-705.
- Santoro, M.; S.R. Shah; J.L. Walker and A.G. Mikos. (2016).** Poly (lactic acid) Nanofibrous Scaffolds for Tissue Engineering,. *Advance Drug Delivery Reviews*, 107:206-212.
- Salami, M.A.; F. Kaveian; M. Rafienia; S. Saber-Samandari; A. Khandan and M. Naeimi. (2017).** Electrospun Polycaprolactone/Lignin-Based Nanocomposite as a Novel Tissue Scaffold for Biomedical Applications. *Journal of Medical Signals and Sensors*, 7: 228-38.
- Singla, R.K.; S.N. Maiti and A.K. Ghosh, (2016).** Crystallization, Morphological and Mechanical response of Poly (lactic acid)/Lignin Based Biodegradable Composite. *Polymer-Plastics Technology and Engineering*, 55(5): 475-485.
- Seo, D.K.; J.P. Jeun; H.B. Kim and P.H. Kang. (2011).** Preparation and Characterization of the Carbon Nano Fiber Mat Produced from Electrospun PAN/Lignin Precursor by Electron Beam Irradiation. *Reviews on Advanced Materials*, 28: 31-34.
- Spiridon, L and Tanase ,C.E. (2018).** Design, Characterization and Preliminary Biological Evaluation of New Lignin-PLA Composites. *International Journal of Biological Macromolecules*, 114: 855-863.
- Spiridon, L.; K. Leluk; A.M. Resmerita, and R.N. Darie. (2015).** Evaluation of PLA-Lignin Bioplastics Properties Before and After Accelerated Wearhering. *Composites part B. Engineering*, 342-349.
- Stanley, J.N.G.; M. Seiva; A.F. Masters; T. Maschmeyer and A. Perosa. (2013).** Reactions of p-coumaryl Alcohol Model Compounds with Dimethyl Carbonate. Towards the Upgrading of Lignin Building Blocks. *Green Chemistry*, 15:3195 – 3204.
- Sun, R.C.; O. Lu and X.F. Sun. (2001).** Physico-chemical and Thermal Characterization of Lignin from *Caligonum Monogolicum* and *Tamarix*. *Supp. Polymer Degradation and Stability*, 72:229-238.
- Tian, D.; X. Zhang; C. Lu; G. Yuang; W. Zhang and Z. Zhou. (2014).** Solvent- Free Synthesis of Carboxylate-Functionalized Cellulose from Waste Cotton Fabrics for the Removal of Cationic Dyes from Aqueous Solutions, *Cellulose*,21: 473-84.
- Vink, E.T.; K.R. Ra'bago; D.A. Glassner; B. Springs; R.P.O. Connor; J. Kolstad, and P.R. Gruber. (2004).** The Sustainability of Natureworks Poly(lactide) Polymers and Ingeo Poly(lactide) Fibers: An Update of the Future. *Molecular Bioscience*, 4: 551–564.
- Wang, H.; Y. Pu; A. Ragauskas and B. Yang. (2019).** **From Lignin to Valuable Products-Strategies, Challenges and Prospects. *Bioresource Technology*. 271;449-461.**
- Wang, K.; S. Bauer and R. Sun. (2012).** Structural Transformation of *Miscanthus Xgiganteus* Lignin Fractionated Under Mild Formosolv, Basic Organosolv and Cellulolytic Enzymes Conditions. *Agricultural Food Chemistry*, 60:144-152.
- Wang, Y.; R. Xu; G. Luo; Q. Lei; Q. Shu; Z. Yao; H. Li; J. Zhou; J. Tan; S. Yang; R. Zhan; W. He and, J. Wu. (2016).** Biomimetic Fibroblast-Loaded Artificial Dermis With Sandwich Structure and Designed Gradient Pore Sizes Promote Wound Healing by Favouring Granulation Tissue

Formation and Wound Re-epitheliazation. *Acta Biomateriala*, 30:246-257.

Zeltinger, J.; J.K. Sherwood; D.A. Graham; R. Mueller and L.G. Griffith. (2001). Effect of Pore Size and Void Fractions on Cellular Adhesion, Proliferation and Matrix Deposition. *Tissue Engineering*, 7:557-572.